Korean J. Chem. Eng., 39(9), 2324-2333 (2022)
DOI: 10.1007/s11814-022-1161-9

pISSN: 0256-1115
eISSN: 1975-7220

Pseudo-homogeneous kinetic modeling of dioctyl terephthalate (DOTP) production by esterification of terephthalic acid and 2-ethylhexanol over tetrabutyl titanate catalyst

Feng Zhou, Jinjin Cai, Xiaoning Mao, Zhenyu Wu, and Yong Nie†

Biodiesel Laboratory of China Petroleum and Chemical Industry Federation, Zhejiang Provincial Key Laboratory of Biofuel, and College of Chemical Engineering, Zhejiang University of Technology, Hangzhou 310014, China
(*Received 12 January 2022 • Revised 26 April 2022 • Accepted 28 April 2022*)

Abstract−As a green plasticizer, the industrial production of dioctyl terephthalate (DOTP) is still facing the problem of high energy consumption. To optimize the production process and reactor, it is essential to understand the kinetic behavior of reaction system. In this work, the two-step consecutive esterification of solid terephthalic acid (PTA) and 2-ethylhexanol (2-EH) catalyzed by tetrabutyl titanate was studied. First, the equilibrium constants and enthalpies of the two-step reaction were experimentally determined and validated by the group contribution methods. Then, a pseudo-homogeneous kinetic model was developed, and the reaction order of PTA was corrected to reflect its solid phase characteristic. Non-isothermal kinetic experiments were carried out under different initial feed molar ratios and catalyst concentrations, and the kinetic parameters in the model were estimated by mathematical regression. The model predicted data agreed well with the experimental data. Finally, the analyses of reaction rate showed that the first-step reaction was the rate-controlling step of the whole esterification process.

Keywords: Heterogeneous Reaction, Esterification, Kinetics, Terephthalic Acid, 2-Ethylhexanol

INTRODUCTION

A plasticizer, as a kind of material that can increase the plasticity and flexibility of polymer materials, is widely used in the plastic industry [1]. At present, the global annual consumption of plasticizer is about 8.5 million tons, and it is expected to reach 10.5 million tons in 2026 [2]. Among them, phthalic acid esters (PAEs) plasticizers have accounted for the majority of the plasticizer market. However, due to health and environmental problems, the applications of PAEs plasticizers have been gradually restricted [3-5]. For example, the US Environmental Protection Agency and the European Union have banned the use of PAEs plasticizers in children and medical supplies [6]. Accordingly, the use of non-toxic and environmentally-friendly plasticizers has become a development trend. Among which, dioctyl terephthalate (DOTP), as a "green" plasticizer, has gradually become an excellent substitute for PAEs plasticizers due to its excellent properties, such as low volatility, lower viscosity, non-carcinogenicity and high electrical resistance [7]. At present, DOTP has become one of the plasticizers with the most investment in the United States [8], Europe [9] and Russia [10].

The production methods of DOTP can generally be divided into three categories: 1) direct esterification of terephthalic acid (PTA) with 2-ethylhexanol (2-EH) [11]; 2) alcoholysis of polyethylene terephthalate (PET) with 2-EH [12]; 3) transesterification of dimethyl terephthalate (DMT) with 2-EH [13]. In industry, the direct esterification of PTA and 2-EH is mainly adopted for the production of DOTP, due to the advantages of abundant raw materials and great product quality [14]. The reaction process of direct esterification is shown in Fig. 1. It is a two-step consecutive reaction. First, mono-2-ethylhexyl terephthalate (MEHTP) is obtained by esterification of PTA and 2-EH in the presence of catalyst. Then, the MEHTP further reacts with 2-EH to produce DOTP. Note that PTA is almost insoluble in liquid-phase system at the reaction temperature [15], which makes the first-step reaction a liquid-solid heterogeneous process.

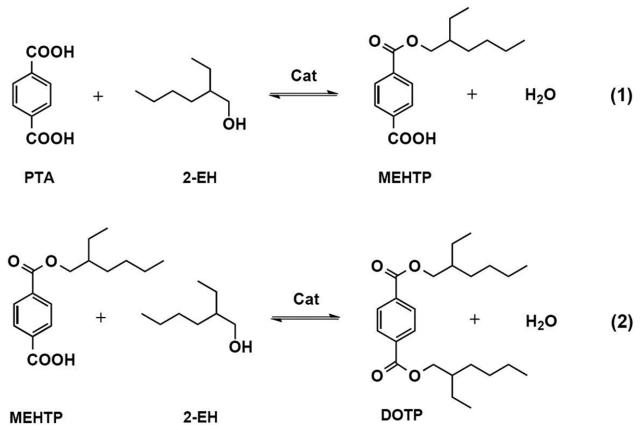

Fig. 1. Esterification of terephthalic acid and 2-ethylhexanol.

In the selection of catalyst, strong acid catalysts, such as sulfuric acid and p-toluenesulfonic acid, were usually used to produce DOTP in the past [14]. However, they were gradually phased out due to corrosion of equipment and generation of waste acid. However, tetra-

†To whom correspondence should be addressed.
E-mail: ny_zjut@zjut.edu.cn

butyl titanate ($Ti(OBu)_4$) has been widely used in various esterification reactions and transesterification reactions due to its excellent catalytic activity and environmental friendliness [16-19]. Meanwhile, $Ti(OBu)_4$ has become one of the main catalysts for the industrial production of DOTP [20].

At present, the industrial production of DOTP by direct esterification of PTA and 2-EH is usually carried out in a reactive distillation unit, due to the reversibility of the esterification reaction. In this process, a great deal of heat is consumed to ensure the generated H_2O in the reactions can be removed in time. In addition, the esterification will be completed in about eight hours in industry, while only about five hours is needed in a lab scale unit under the same reaction conditions. It indicates that the existing reactors of DOTP production still have considerable room for optimization in enhancing mass and heat transfer rate. Therefore, optimizing process parameters and designing novel reactors have practical economic significance for DOTP industry production.

It is known that reaction kinetics is the basis for process optimization and reactor design. In the past few decades, only a few reports have studied the kinetics of this esterification. Wei et al. [21] studied the esterification mechanism and the kinetic parameters of the esterification of PTA and 2-EH, where the two reactions are treated as irreversible ones. They found that the ratio of the rate constants of the two reactions k_2/k_1 is about 19. Li et al. [22] studied the esterification of PTA and 2-EH using $Ti(OBu)_4$ as catalyst. They simplified the two-step reaction into a one-step reaction and obtained activation energy of 95.52 $kJ\cdot mol^{-1}$. As can be seen from the literature survey, the simplification of key properties, such as reversibility and two-step reaction, has made the models less universal. Hence, it is necessary to establish an accurate and systematic kinetic model for the esterification of PTA and 2-EH.

In this study, the kinetic behavior of esterification of PTA and 2-EH catalyzed by $Ti(OBu)_4$ was systematically investigated. First, the equilibrium constants and enthalpies of the two-step reaction at different reaction temperatures were investigated. Then, kinetic experiments were carried out under different feed molar ratios, catalyst concentrations and temperature ranges, and the kinetic parameters were determined using nonlinear regression method. The accuracy and applicability of the kinetic model were further verified by error analyses and random experiments. Finally, the rate-controlling step of the esterification was analyzed by the obtained kinetic model.

EXPERIMENTAL

1. Materials

PTA (99%, AR) was purchased from Aladdin company. 2-EH (99%, AR) was purchased from Macklin company. $Ti(OBu)_4$ (99%, AR) was purchased from Sinopharm Chemical Reagent Co. Ltd. Ethanol (99.8%, HPLC) and acetonitrile (99.9%, HPLC) for chromatographic analysis were purchased from Adamas Reagent, Ltd.

2. Analysis

2-EH and DOTP were analyzed using a gas chromatographic system (GC-2014C, Shimadzu) equipped with a flame ionization detector (FID) and a DB-5 column (30 m×0.25 mm×0.25 μm, Agilent). The temperature of the gasification chamber and the detector was set as 563.15 K. The column temperature program was as follows: the initial temperature was 423.15 K, then heated to 463.15 K at a rate of 5 $K\cdot min^{-1}$, and then heated to 553.15 K at a rate of 10 $K\cdot min^{-1}$, and held at 553.15 K for 8 mins. High-purity nitrogen (>99.99%) served as carrier gas.

MEHTP was analyzed using an HPLC system (LC-20AT, Shimadzu) equipped with a refractive index detector (RID) and a C18 column (30 m×0.25 mm×0.25 μm, Silgreen). The oven temperature was 318.15 K, and the mobile phase flow rate was maintained as 0.8 $ml\cdot min^{-1}$ using a mixture of 15 wt% water and 85 wt% acetonitrile.

Water in the liquid phase system was analyzed by Karl Fischer titration (870 KF Titrino Plus, Metrohm).

To determine the concentration of each component, the mass of liquid in the system m_l should be determined first. It is worth noting that m_l was gradually increasing with the conversion of PTA in the reaction process. Here, m_l during the reaction can be calculated based on the mass balance of 2-EH:

$$\frac{m_l\cdot\omega_{2\text{-}EH}}{M_{2\text{-}EH}}=n^0_{2\text{-}EH}-\frac{2m_l\cdot\omega_{DOTP}}{M_{DOTP}}-\frac{m_l\cdot\omega_{MEHTP}}{M_{MEHTP}} \tag{1}$$

After an algebraic rearrangement, m_l can be expressed as following:

$$m_l=n^0_{2\text{-}EH}\left(\frac{\omega_{2\text{-}EH}}{M_{2\text{-}EH}}+\frac{2\omega_{DOTP}}{M_{DOTP}}+\frac{\omega_{MEHTP}}{M_{MEHTP}}\right)^{-1} \tag{2}$$

where n_i^0 is the initial molar number of component *i*, M_i is the molar mass of component *i*, ω_i is the mass fraction of component *i* in the liquid system. Then, the molar number n_i and the concentration of each component C_i in the liquid system can be obtained:

$$n_i=\frac{m_l\cdot\omega_i}{M_i} \tag{3}$$

$$C_i=\frac{n_i}{V_{sys}} \tag{4}$$

where is the volume of reaction system, which was assumed to be constant during the reaction.

For solid PTA, we assumed it is completely insoluble and performed pseudo-homogenization treatment on it. The concentration of PTA can be determined by the following:

$$C_{PTA}=\frac{n^0_{PTA}-n_{DOTP}-n_{MEHTP}}{V_{sys}} \tag{5}$$

3. Chemical Equilibrium Experiments

The chemical equilibrium experiments were carried out in a 250 mL stainless steel high-pressure reactor as shown in Fig. 2. The reactor adopted modular design, including a heating jacket, a pressure meter (accuracy ±0.1 MPa, with pressure safety valve), a Pt100 needle temperature sensor (accuracy ±0.1 K), a mechanical stirrer (0-1,500 rpm), a 100 ml feed system and multiple control valves.

Initially, the reactor was sealed with a certain feed molar ratio, and high-purity nitrogen was pumped into the reactor through a nitrogen cylinder. The system pressure in the reactor was adjusted to 3 MPa to avoid the gasification of H_2O and 2-EH at reaction temperature (the saturated vapor pressure of the azeotrope of H_2O and

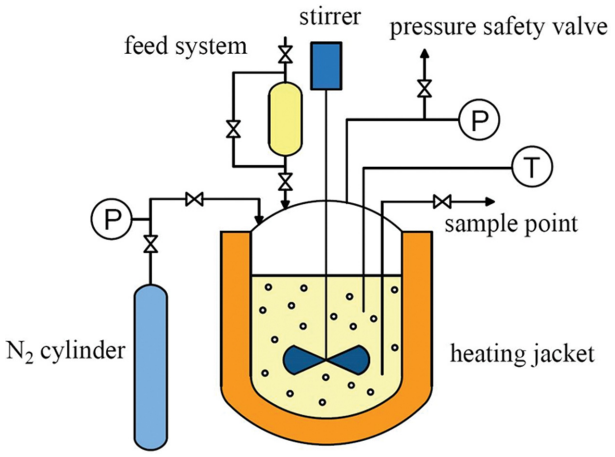

Fig. 2. Structure diagram of equipment used for chemical equilibrium experiments.

2-EH is 2 MPa at the maximum reaction temperature of 483.15 K). Then, catalyst was added through the feed system under a stirring speed of 500 rpm when system temperature reached the set value. Samples were taken through the sampling point at regular intervals and immediately cooled for analysis. The reaction was considered to have reached equilibrium when the concentration variation of adjacent samples was less than 3%.

4. Kinetic Experiments

The equipment used for kinetic experiments is as shown in Fig. 3. It can be divided into a reaction unit and a reflux unit. In the reaction unit, the esterification of PTA and 2-EH was carried out in a 250 mL four-necked flask equipped with heating jacket, stirrer, and thermometer. The gaseous mixture of 2-EH and H_2O can enter the reflux unit through the connecting pipe under the condition of heat preservation. In the reflux unit, the gaseous mixture was condensed and stratified, H_2O sank to the bottom, and the upper 2-EH overflowed back to the reaction unit.

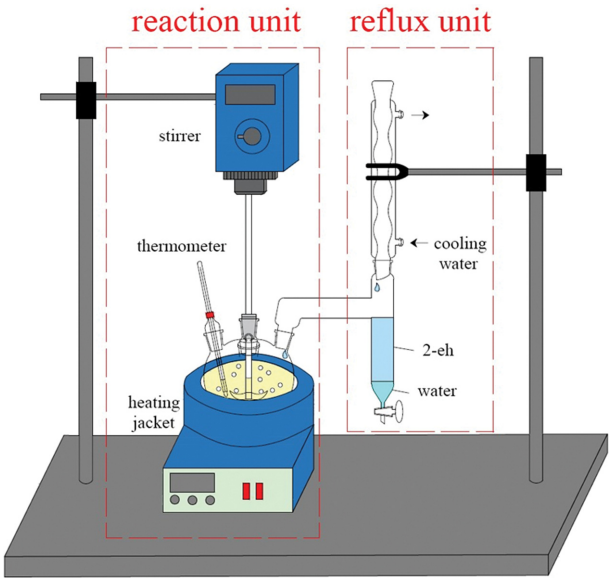

Fig. 3. Scheme of equipment used for kinetic experiments.

Table 1. Experimental matrix for esterification kinetics[a]

Run	Feed molar ratio of PTA and 2-EH	Concentration of catalyst ($mol \cdot L^{-1}$)
1	1 : 3	0.0015
2	1 : 3	0.0030
3	1 : 4	0.0030
4	1 : 5	0.0030
5	1 : 3	0.0045
6	1 : 4.5	0.0030

[a]Feed molar ratio and concentration of catalyst were selected within the general range of DOTP industrial production.

A typical experimental procedure was as follows: a certain amount of PTA and 2-EH were first added into the flask, and the reflux unit was filled with 2-EH. A certain amount of catalyst was added at a certain stirring speed when the temperature reached 453.15 K, and the moment of addition was taken as time zero of the reaction. During the reaction, the H_2O at the bottom of the reflux unit was discharged at regular intervals to ensure the mass balance of 2-EH in the flask. The system temperature depended on the bubble point temperature of the liquid mixture, which was gradually increased with the formation of esters. We sampled at regular intervals and recorded the system temperature.

To eliminate the mass transfer limitation, the effects of PTA particle size and stirring speed were first investigated. PTA was sieved and divided into 90-100, 140-150 and 190-200 mesh, the stirring speed was investigated from 100 to 400 rpm.

Kinetic experiments were carried out under the condition of eliminating mass transfer limitation. The experimental matrix for esterification kinetics is shown in Table 1. Run 1 to run 4 were used to regress the kinetic parameters, run 4 and run 5 were used to verify the accuracy and applicability of obtained parameters.

RESULTS AND DISCUSSION

1. Chemical Equilibrium Constants and Enthalpies of Reactions

In the initial feeding stage of equilibrium experiments, a certain amount of DOTP and excessive catalyst was added in the reactor to reduce the overall equilibrium time. The time evolutionary profiles of concentration at two typical temperatures in the equilibrium experiments are shown in Fig. 4. As can be seen, the concentration of each component remained almost unchanged when the reaction time was above 10 h. Hence, the following equilibrium constants in this work were calculated based on the data at 12 h.

The chemical equilibrium constants for the two-step reaction K_1 and K_2 can be expressed as follows:

$$K_1 = \frac{C^{eq}_{MEHTP} C^{eq}_{H_2O}}{C^{eq}_{2\text{-}EH}} \tag{6}$$

$$K_2 = \frac{C^{eq}_{DOTP} C^{eq}_{H_2O}}{C^{eq}_{MEHTP} C^{eq}_{2\text{-}EH}} \tag{7}$$

where C_i^{eq} is the equilibrium molar concentration of component *i*.

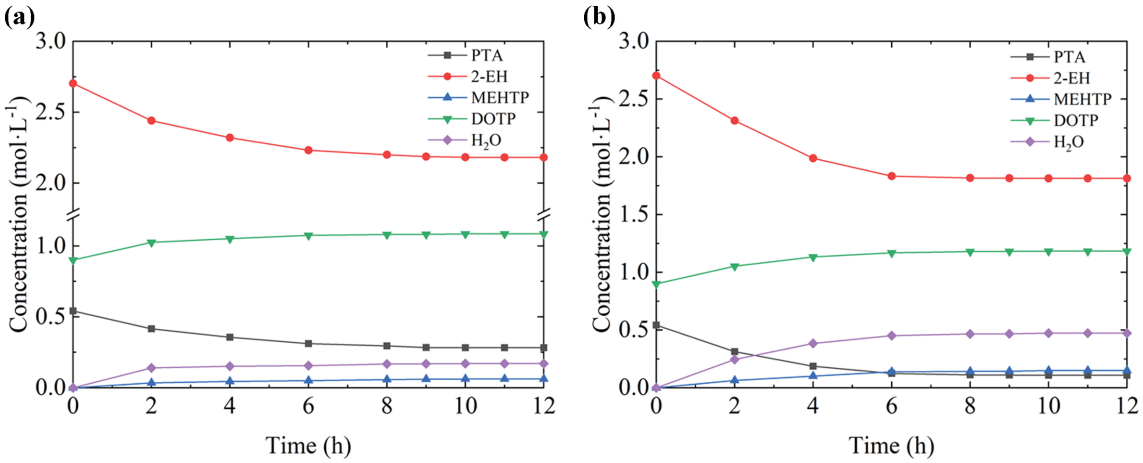

Fig. 4. Time evolutionary profiles of the concentration at typical temperatures in equilibrium experiments (a) 453.15 K; (b) 483.15 K.

Table 2. Chemical equilibrium constants at different temperatures

Temperature (K)	K_1	K_2
453.15	0.0062	1.303
463.15	0.0074	1.557
473.15	0.0178	1.916
483.15	0.0391	2.061

The values of K_1 and K_2 at different temperatures are listed in Table 2. The results show that K_1 was 0.0062-0.0391 at a reaction temperature range from 453.15 to 483.15 K, while K_2 was 1.303-2.061 at the same conditions. It indicates that the first-step reaction is severely constrained by the chemical equilibrium. Therefore, the timely removal of H_2O during the reaction is essential to improve the conversion of PTA.

The temperature dependence of the equilibrium constants reflected the enthalpy of reaction ΔH_r and ΔH_r can be calculated by van't Hoff equation as Eq. (8):

$$\frac{d\ln K}{d\frac{1}{T}} = \frac{-\Delta H_r}{R} \tag{8}$$

where R is the gas constant with a value of 8.314 J·mol^{-1}·K^{-1}.

Fig. 5 shows the relationship between lnK and 1/T of the two-step reaction. The enthalpies of the two-step reaction, obtained from the slope of the trend lines in Fig. 4, were 115.81 kJ·mol^{-1} for the first-step reaction (ΔH_{r1}) and 28.89 kJ·mol^{-1} for the second-step reaction (ΔH_{r2}). The results indicate the strong endothermic property of the whole esterification. The value of ΔH_{r1} is much larger than that of ΔH_{r2}, it may be related to the phase state difference between PTA and MEHTP at reaction temperature.

It should be noted that C^{eq}_{MEHTP} and $C^{eq}_{H_2O}$ in chemical equilibrium experiments were quite low, so the analytical errors may have a certain effect on the experimental results of ΔH_r. To further verify the accuracy of ΔH_r, the group contribution methods were adopted to estimate the enthalpies of reactions and compared with the experimental data.

The standard enthalpy of reaction $\Delta H^0_{r,T}$ was calculated as:

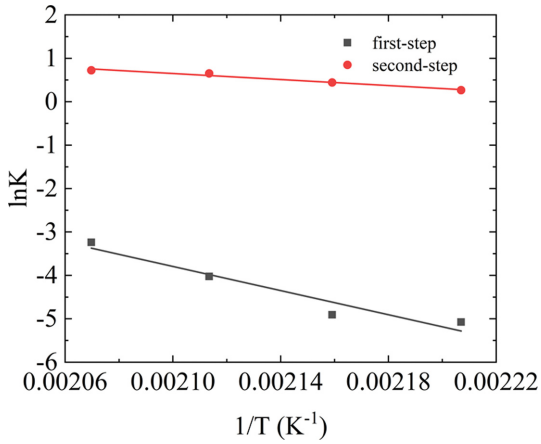

Fig. 5. Relationship between 1/T and lnK of the two-step reaction.

$$\Delta H^0_{r,T} = \sum \upsilon_i \cdot \Delta H^0_{fi,T} \tag{9}$$

$$\Delta H^0_{fi,T} = \Delta H^0_{fi,298.15\,K} + \int_{298.15}^{T} C_{pi,T}\,dT \tag{10}$$

where υ_i is stoichiometric coefficient of component *i*, $\Delta H^0_{fi,T}$ is standard enthalpy of formation of component *i*, $C_{pi,T}$ is the constant pressure heat capacity of component *i*.

In the standard state (100 kPa), the reaction temperature far exceeds the boiling point of H_2O, so the H_2O generated in the reactions can be considered as a gaseous state. The $\Delta H^0_{f,298.15\,K}$ and $C_{p,T}$ of PTA, 2-EH and H_2O were obtained from the literature [23-27]. The $C_{p,T}$ of MEHTP and DOTP were estimated by the group contribution method proposed by Rozicka and Domalski [28]. Note that the $\Delta H^0_{f,298.15\,K}$ of liquid component cannot be estimated directly. Therefore, the $\Delta H^0_{f,298.15\,K}$ of liquid MEHTP and DOTP were calculated as:

$$\Delta H^0_{fi,298.15\,K} = \Delta H^0_{fg,298.15\,K} - \Delta H^0_{vap,298.15\,K} \tag{11}$$

where $\Delta H^0_{fi,298.15\,K}$ is standard enthalpy of formation of liquid component at 298.15 K. $\Delta H^0_{fg,298.15\,K}$ is standard enthalpy of formation of gas component at 298.15 K, which was estimated by the group contribution method proposed by Benson [29]. $\Delta H^0_{vap,298.15\,K}$ is

Table 3. Estimated thermodynamic parameters of components

Component	$\Delta H^0_{fg,\,298.15\,K}$ (kJ·mol^{-1})	$\Delta H_{vap,\,298.15\,K}$ (kJ·mol^{-1})	$\Delta H_{vap,\,b}$ (kJ·mol^{-1})	T_b (K)	T_c (K)
MEHTP	−818.33	83.29	57.19	692.13	916.67
DOTP	−964.34	100.57	66.86	739.45	969.69
PTA (liquid)	−672.32	62.34	46.00	507.66	679.73

Component	$C_{p,\,T}=8.314(A+BT10^{-2}+CT^2 10^{-4})$ (J·mol^{-1}·K^{-1})		
	A	B	C
MEHTP	37.41	3.88	1.23
DOTP	63.47	1.53	2.08
PTA (liquid)	11.34	6.23	0.38

Table 4. Estimated values of $\Delta H^0_{r,\,T}$ and $\Delta H^0_{f,\,T}$ at different temperatures

Temperature (K)	$\Delta H^0_{r1,\,T}$ (kJ·mol^{-1})	$\Delta H^0_{r2,\,T}$ (kJ·mol^{-1})	$\Delta H^0_{f,\,T}$ (kJ·mol^{-1})	
			PTA (liquid)	PTA (solid)
453.15	114.00	15.41	−682.98	−785.23
463.15	115.32	14.76	−679.01	−783.23
473.15	116.71	14.10	−674.96	−781.24
483.15	118.17	13.42	−670.82	−779.24

enthalpy of vaporization of liquid component at 298.15 K which was calculated by the Watson equation [30] expressed as follows:

$$\Delta H_{vap,\,T}=\Delta H_{vap,\,b}\left(\frac{1-T_r}{1-T_{br}}\right)^n \tag{12}$$

$$T_r=\frac{T}{T_c} \tag{13}$$

$$T_{br}=\frac{T_b}{T_c} \tag{14}$$

$$n=\left(\frac{0.00264\Delta H_{vap,\,b}}{RT_b}+0.8794\right)^{10} \tag{15}$$

where $\Delta H_{vap,\,b}$ is enthalpy of vaporization of liquid component at the normal boiling point, which was estimated by the group contribution method proposed by Ma [31]; the boiling point T_b and the critical temperature T_c were estimated by M-P group contribution method [32].

To verify the effect of PTA phase state on the enthalpy of first-step reaction, the thermodynamic parameters of PTA (liquid) were also estimated by the above method. The estimated thermodynamic parameters of MEHTP, DOTP and PTA (liquid) are listed in Table 3, and the specific calculation process can be seen in the supplementary materials. Table 4 lists the estimated $\Delta H^0_{r,\,T}$ of the two-step reaction at different temperatures. It can be seen that $\Delta H^0_{r,\,T}$ of the two-step reaction was less dependent on temperature, and the average values of ΔH^0_{r1} and ΔH^0_{r2} at the reaction temperature range were estimated to be 116.05 kJ·mol^{-1} and 14.42 kJ·mol^{-1}, respectively. The result of theoretical analysis was consistent with the experimental conclusion that first-step reaction is highly endothermic and second-step reaction is weakly endothermic. Moreover, the estimated $\Delta H^0_{f,\,T}$ of PTA (liquid) and PTA (solid) at different temperatures are also listed in Table 4. As can be seen, the difference between $\Delta H^0_{r1,\,T}$ and $\Delta H^0_{r2,\,T}$ is almost equal to the difference between the $\Delta H^0_{f,\,T}$ of PTA (liquid) and PTA (solid), which indicates that the high value of ΔH^0_{r1} can be considered as containing the melting enthalpy of PTA. It further verifies that the high endothermic property of the first-step reaction was due to the solid phase states of PTA under reaction conditions.

2. Kinetic Modeling

2-1. Elimination of Mass Transfer Limitation

Fig. 6 shows the relationship between PTA conversion and time at different stirring speeds. As can be seen, the reaction rate was improved by increasing stirring speed in a certain range. When the stirring speed was above 200 rpm, the mass transfer limitation of reactions could be eliminated. Fig. 7 shows the relationship between PTA conversion and time at different PTA particle sizes. The result

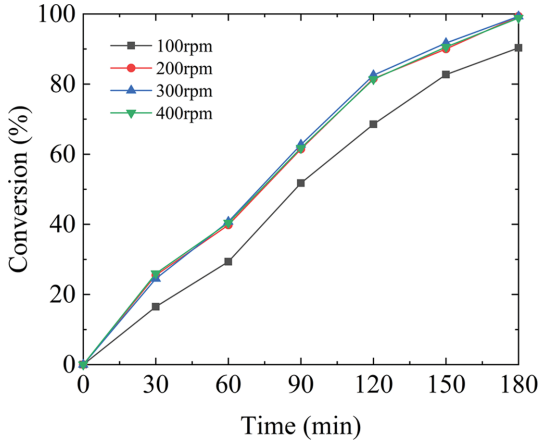

Fig. 6. Effect of the stirring speed on the conversion of PTA.

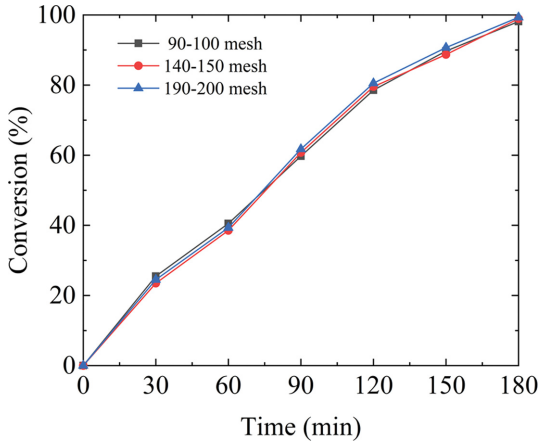

Fig. 7. Effect of the PTA particle size on the conversion of PTA.

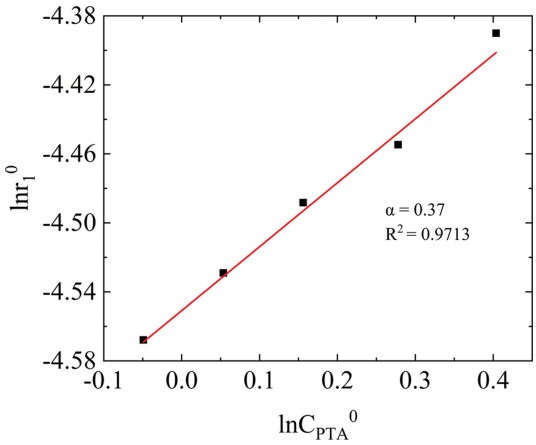

Fig. 8. Relationship between $\ln r_1^0$ and $\ln C_{PTA}^0$.

indicates that the particle size of PTA, at the range of 90-200 mesh, almost has no effect on the conversion of the PTA. Hence, the esterification experiments in the following sections were performed at 400 rpm, and the purchased PTA can be directly used without any pre-treatment.

2-2. Kinetic Equations

Generally, esterification reactions follow a first-order contribution of each component to the reaction rate [33,34]. However, the rate equations of the esterification of insoluble acid are more complex than that of the homogeneous reactants [35]. Hence, for the esterification of PTA and 2-EH, the solid phase characteristic of PTA was reflected by correcting the reaction order of PTA. The rate equations for the two-step reaction are expressed as follows:

$$r_1 = k_1 C_{cat}\left(C_{PTA}{}^{\alpha} C_{2\text{-}EH} - \frac{1}{K_1} C_{MEHTP} C_{H_2O}\right) \tag{16}$$

$$r_2 = k_2 C_{cat}\left(C_{MEHTP} C_{2\text{-}EH} - \frac{1}{K_2} C_{DOTP} C_{H_2O}\right) \tag{17}$$

where α is the reaction order of PTA. k_i and K_i are the forward reaction rate constants and the equilibrium constants, respectively.

The value of α was determined by the initial rate method as follows: esterification experiments were carried out at different initial C_{PTA}, the trend lines of C_{PTA} were obtained by polynomial fitting of the experimental data and the R-squared of each trend line was above 0.99. The negative of the time derivative of the trend lines at the initial time $\left(-\frac{dC_{PTA}}{dt}\right)^0$ was the initial reaction rate of the first-step reaction r_1^0, and r_1^0 can be expressed as follows:

$$r_1^0 = k_1^0 C_{cat}\left(C_{PTA}{}^{\alpha} C_{2\text{-}EH}^0 - \frac{1}{K_1} C_{MEHTP}^0 C_{H_2O}^0\right) \tag{18}$$

where k_1^0 is the forward reaction rate constant of the first-step reaction at initial temperature. C_i^0 is the initial concentration of component *i*.

In the experiments, the C_{MEHTP}^0 and $C_{H_2O}^0$ were zero, hence Eq. (18) can be simplified as:

$$r_1^0 = k_1^0 C_{cat} C_{PTA}^0{}^{\alpha} C_{2\text{-}EH}^0 \tag{19}$$

Take the logarithm of both sides of Eq. (19) to get the following equation:

$$\ln r_1^0 = \ln k_1^0 + \ln C_{cat} + \alpha \ln C_{PTA}^0 + \ln C_{2\text{-}EH}^0 \tag{20}$$

Since C_{cat}, $C_{2\text{-}EH}^0$ and k_1^0 in Eq. (20) are constant, the above equation can be further simplified as:

$$\ln r_1^0 = \alpha \ln C_{PTA}^0 + A \tag{21}$$

where $A = \ln k_1^0 + \ln C_{cat} + \ln C_{2\text{-}EH}^0$.

Fig. 8 shows the relationship between $\ln r_1^0$ and $\ln C_{PTA}^0$. The slope of the trend line represents the reaction order of PTA and the value was 0.37. It is normal for the dispersed phase reactant to have a reaction order less than 1, when using a kinetic model based on homogeneous reaction to describe a heterogeneous reaction. Tian et al. [16] also found that the reaction order of PTA was 0.7 in the mono-esterification of PTA and 1,4-Butanediol under homogeneous model. Moreover, similar phenomena have also been found in some gas-liquid heterogeneous systems. Okitsu et al. [36] found that the reaction order of acid was always less than 1 in the sonochemical decomposition of butyric acid and benzoic acid when using homogeneous model.

In the kinetic experiment, the reaction temperature was always the bubble temperature of the liquid system and it gradually increased with the reaction. Due to the low content of MEHTP and H_2O during the reaction, the bubble point temperature of the system was mainly determined by the composition of 2-EH and DOTP. Therefore, the relationship between bubble point temperature and x_{DOTP} of the binary system of 2-EH and DOTP was measured, and a polynomial fitting was performed as shown in Fig. 9. The bubble point temperature when x_{DOTP} above 0.6 was not measured because x_{DOTP} will not exceed 0.6 in kinetic experiments and general industrial production.

The temperature dependence of the rate constant was described using the Arrhenius equation, expressed as:

$$k = k^{ref} \exp\left[\frac{E_a}{RT}\left(\frac{1}{T^{ref}} - \frac{1}{T}\right)\right] \tag{22}$$

where E_a is the activation energy of reaction, T is the absolute temperature, T^{ref} is the reference temperature (here was 453.15 K), k^{ref}

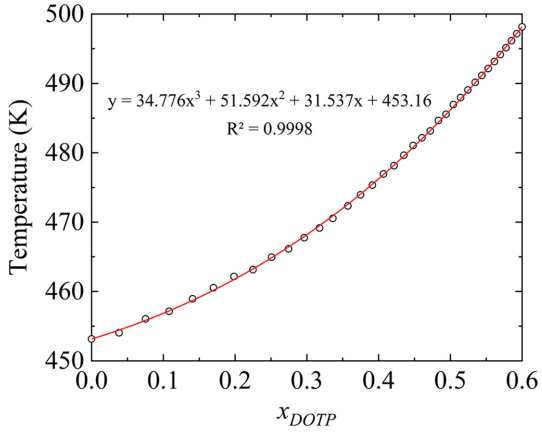

Fig. 9. Relationship between bubble point temperature and x_{DOTP}.

is the forward reaction rate constant at the reference temperature.

The mass balance equation of each component in the reaction can be expressed as:

$$\frac{dC_{PTA}}{dt} = -r_1 \tag{23}$$

$$\frac{dC_{2\text{-}EH}}{dt} = -(r_1 + r_2) \tag{24}$$

$$\frac{dC_{MEHTP}}{dt} = r_1 - r_2 \tag{25}$$

$$\frac{dC_{DOTP}}{dt} = r_2 \tag{26}$$

It should be pointed out that the content of H_2O in the system can be ignored due to the timely removal of H_2O in kinetic experiments. Therefore, the change of C_{H_2O} during reaction can be expressed as:

$$\frac{dC_{H_2O}}{dt} = 0 \tag{27}$$

2-3. Determination of Kinetic Parameters

The kinetic parameters (forward reaction rate constants k and energies of activation E_a) involved in the above kinetic equations were obtained by mathematical regression using the experimental data of run 1 to run 4 in Table 1. The ordinary differential equations were solved using the "ode45" function in MATLAB, and the nonlinear least square package "lsqnonlin" was used to regress parameters.

Fig. 10 shows the calculated data of the model based on corrected PTA order (as model 1) and the experimental data. To reflect the necessity of reaction order correction of PTA, the calculated data of the model based on first-order contribution (as model 2) are also presented in Fig. 10. It can be seen that the calculated data of model 1 show a better agreement with experimental data than that of model 2. In addition, the residual square sum (RSS) between the calculated and experimental data was used to quantitatively reflect the accuracy of model, which was calculated as:

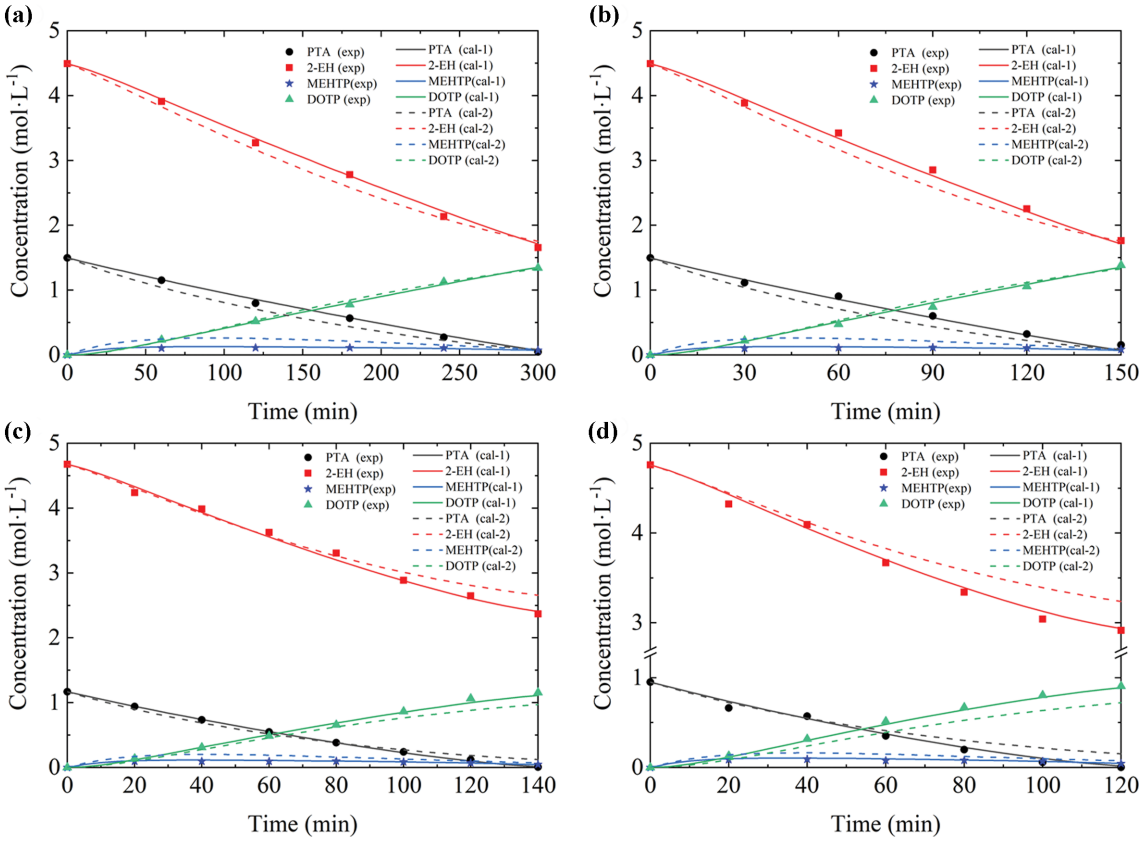

Fig. 10. Experimental and calculated molar concentrations of each component for runs 1-4.

Table 5. Kinetic parameters of the two-step reaction at 453.15 K

Parameter	Value	Relative deviation	Unit
k_1	0.785±0.040	5%	$mol^{-1.37}\cdot L^{1.37}\cdot min^{-1}$
k_2	6.222±2.119	34%	$mol^{-1.37}\cdot L^{1.37}\cdot min^{-1}$
E_{a1}	98.60±15.67	16%	$kJ\cdot mol^{-1}$
E_{a2}	85.51±67.24	78%	$kJ\cdot mol^{-1}$

$$RSS=\Sigma_i^{nc}\Sigma_i^{nt}(C_{i,cal}-C_{i,exp})^2 \quad (28)$$

where nc and nt are the number of component and time point, $C_{i,cal}$ and $C_{i,exp}$ are the calculated and experimental molar concentrations of component *i*, respectively. The RSS values of the two models were 0.1418 and 1.1164, respectively. Therefore, compared with the kinetic model based on first-order contribution, the model based on corrected PTA order can better reflect the real reaction process and predict the reaction process more accurately. Especially under the condition of high 2-EH content, the model based on the first-order contribution showed a large deviation between the experimental and calculated data in the late stage of the esterification. Braam et al. [37] also found this phenomenon, and believed that the larger deviation between the experimental and calculated data at a high conversion was due to the solubility difference of insoluble acids at different temperatures.

The kinetic parameters at 453.15 K obtained in the above regression analyses are listed in Table 5. The kinetic parameters were estimated with a confidence level of 95%, which is the frequency of possible confidence intervals that contain the true value of their corresponding parameters. It can be noticed that the relative deviations of k_2 and E_{a2} were 34% and 78% respectively; the reason is that C_{MEHTP} in the esterification process was quite small, so the errors in measurement of C_{MEHTP} can have a certain influence on the estimate of k_2 and E_{a2}. Moreover, P-value tests were carried out on the experimental and calculated data of each group of experiments. All P-values in obtained model were less than 0.001, further illustrating the significance of statistical analyses.

The applicability of the obtained kinetic model was tested by using two random experiments (run 5 and run 6), and the results are shown in Fig. 11. It was found that the calculated data agreed well with the experimental data, indicating that the obtained model has good applicability and accuracy.

3. Rate-controlling Step

The relationship between forward reaction rate and reaction time under different reaction conditions, which can be obtained from the obtained kinetic model, is shown in Fig. 12. As can be seen, at the initial stage of the esterification, r_1 was significantly larger than r_2, so the second-step reaction was the rate-controlling step at the initial stage of esterification. With the generation of MEHTP and the consumption of PTA, r_2 gradually exceeded r_1 and the first-step reaction became the rate-controlling step. However, the growth rate of r_2 was positively correlated with r_1 at the initial stage of reaction. The faster MEHTP formed, the faster r_2 increased. Therefore, the first-step reaction can be considered as the rate-controlling step in the whole esterification processes. Wei et al. [21] reached the same conclusion by comparing the forward reaction rate constants of the two reactions. Therefore, intensifying the first-step reaction, such as strengthening the liquid-solid mass transfer and water removal, is important to accelerate the whole esterification rate of DOTP industrial production.

CONCLUSIONS

A kinetic study of the esterification of PTA and 2-EH by using tetrabutyl titanate as catalyst was performed. Independent experiments were designed to investigate the equilibrium constants of the two-step reaction at 453.15-483.15 K, and their value ranges were 0.0062-0.0391 and 1.303-2.061, respectively. The enthalpies of the two-step reaction were 115.81 $kJ\cdot mol^{-1}$ and 28.89 $kJ\cdot mol^{-1}$, which were further verified by the group contribution methods. Then, a kinetic model was developed; and the solid phase characteristic of PTA was reflected by correcting the reaction order of PTA and its value was 0.37. The forward reaction rate constants of two reactions k_1 and k_2 at 453.15 K were 0.785 $mol^{-1.37}\cdot L^{1.37}\cdot min^{-1}$ and 6.222 $mol^{-1.37}\cdot L^{1.37}\cdot min^{-1}$, respectively. The activation energies were 98.60 $kJ\cdot mol^{-1}$ and 85.51 $kJ\cdot mol^{-1}$, respectively. The accuracy and applicability of the model was tested by random experiments, and the calculated data showed a great agreement with the experimental

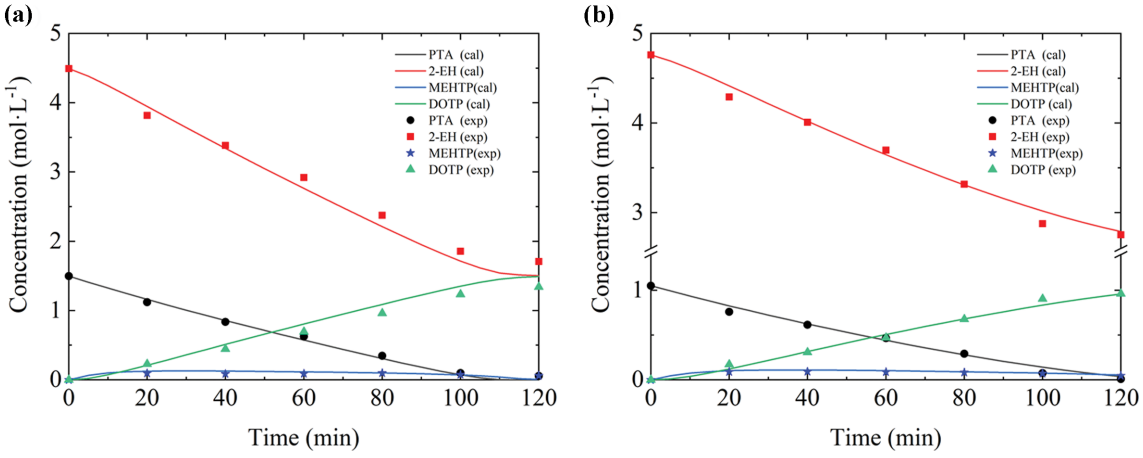

Fig. 11. Experimental and calculated molar concentrations of each component for runs 5-6.

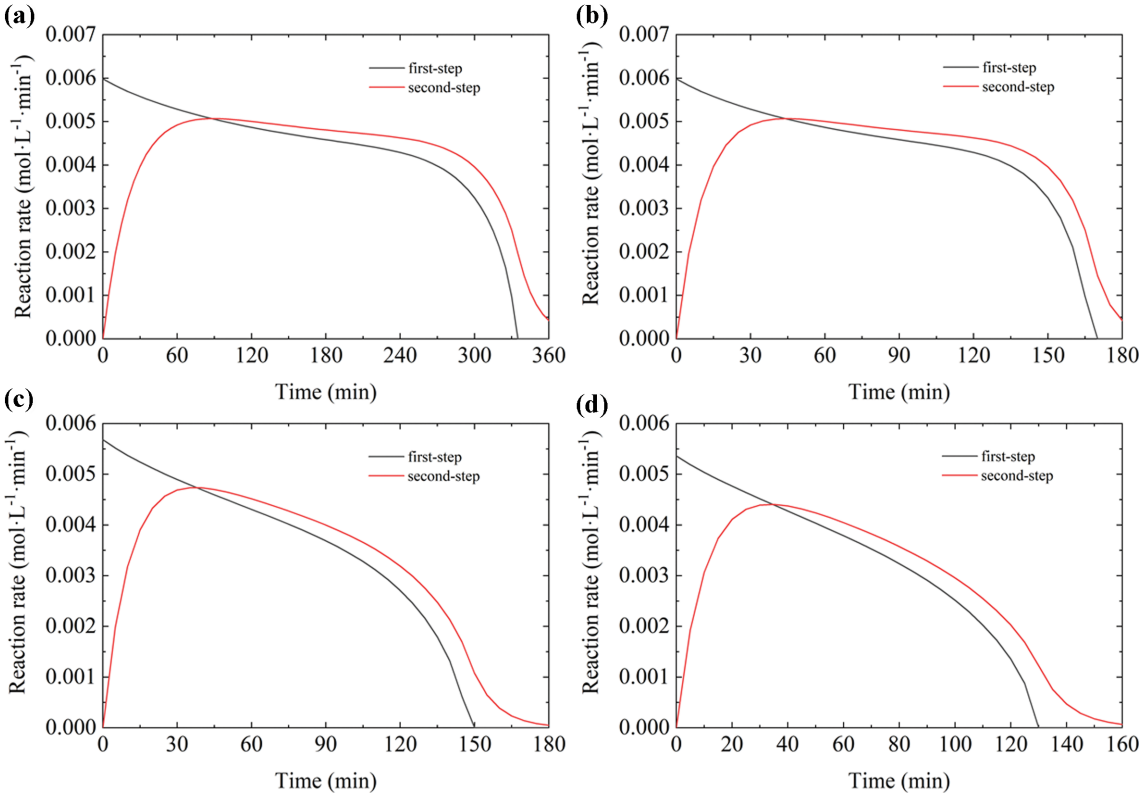

Fig. 12. Relationship between forward reaction rate and reaction time in runs 1-4.

data. Finally, the rate-controlling step was analyzed by the obtained kinetic model, with results showing that the strengthening of first-step reaction is the key to accelerating the whole esterification reaction.

NOMENCLATURE

2-EH : 2-ethylhexanol
PTA : terephthalic acid
DOTP : dioctyl terephthalate
MEHTP : mono-2-ethylhexyl terephthalate
M_i : molar mass of component *i* [g·mol^{-1}]
C_i : concentration of component *i* [mol·L^{-1}]
C_i^0 : initial concentration of component *i* [mol·L^{-1}]
C_i^{eq} : equilibrium molar concentration of component *i* [mol·L^{-1}]
C_p : constant pressure heat capacity [J·mol^{-1}]
V_{sys} : volume of reaction system [L]
R : gas constant
K : equilibrium constant of reaction
ΔH_r : enthalpy of reaction [kJ·mol^{-1}]
ΔH_r^0 : standard enthalpy of reaction [kJ·mol^{-1}]
ΔH_f^0 : standard enthalpy of formation [kJ·mol^{-1}]
$\Delta H_{vap,T}$: enthalpy of vaporization at temperature T [kJ·mol^{-1}]
$\Delta H_{vap,b}$: enthalpy of vaporization at the normal boiling point [kJ·mol^{-1}]
T : absolute temperature [K]
T^{ref} : reference temperature [K]
T_c : critical temperature [K]
T_b : boiling point temperature [K]
E_a : activation energy of reaction [kJ·mol^{-1}]
t : reaction time [min]
r : reaction rate [mol^{-1}·L^{-1}·min^{-1}]
r^0 : initial reaction rate [mol^{-1}·L^{-1}·min^{-1}]
k : forward reaction rate constants [mol$^{-1.37}$·L$^{1.37}$·min^{-1}]
k^{ref} : forward reaction rate constant at the reference temperature [mol$^{-1.37}$·L$^{1.37}$·min^{-1}]
m_l : mass of liquid in the system [g]
n_i^0 : initial molar number of component *i* [mol]
υ_i : stoichiometric coefficient of component *i*
α : reaction order of PTA
ω_i : mass fraction of component *i*
x_{DOTP} : mole fraction of DOTP

SUPPORTING INFORMATION

Additional information as noted in the text. This information is available via the Internet at http://www.springer.com/chemistry/journal/11814.

REFERENCES

1. M. Park, I. Choi, S. Lee, S. Hong, A. Kim, J. Shin, H C. Kang and Y. W. Kim, *J. Ind. Eng. Chem.*, **88**, 148 (2020).
2. Ceresana's latest report details growth and change for global plasticizers market, *Addit. Polym.*, 11 (2019).
3. J. L. Lyche, A. C. Gutleb, Å. Bergman, G. S. Eriksen, A. J. Murk, E. Ropstad, M. Saunders and J. U. Skaare, *J. Toxicol. Environ. Heal. -*

Part B Crit. Rev., **12**, 225 (2009).
4. S. Net, R. Sempéré, A. Delmont, A. Paluselli and B. Ouddane, *Environ. Sci. Technol.*, **49**, 4019 (2015).
5. Y. F. Miao, R. H. Wang, C. Lu, J. P. Zhao and Q. H. Deng, *Environ. Sci. Pollut. Res.*, **24**, 312 (2017).
6. H. C. Erythropel, T. Brown, M. Maric, J. A. Nicell, D. G. Cooper and R. L. Leask, *Chemosphere*, **134**, 106 (2015).
7. V. A. Küçük, M. Uğur, H. Korucu, B. Şimşek, T. Uygunoğlu and M. M. Kocakerim, *Constr. Build. Mater.*, **263**, 120905 (2020).
8. BASF begins production of dioctyl terephthalate at Texas facility, *Focus Catal*, 6 (2017).
9. Oxea aims to become major European supplier of DOTP plasticizer, *Addit. Polym.*, 7 (2018).
10. A. Jacoby and Z. Adams, *Addit. Polym.*, 8 (2019).
11. K. Du, M. L. Lian, Z. F. Fan and Y. Li, *Appl. Mech. Mater.*, **541**, 95 (2014).
12. J. Y. Ding, J. Y. Chen, Y. M. Ji, P. Ni, Z. L. Li and L. Y. Xing, *J. Anal. Appl. Pyrolysis*, **106**, 99 (2014).
13. S. T. Firdovsi, M. Yagoub and A. E. Parvin, *Chinese J. Chem.*, **25**, 246 (2007).
14. P. P. Jiang, Q. F. Zhang, W. Gao, P. B. Zhang, Y. M. Dong, Y. Leng, C. C. Sun, Y. H. Liu and Y. B. Chen, *Plast. Addit.*, **137**, 9 (2019).
15. D. Celante, L. O. Diehl, L. N. Brondani, C. A. Bizzi and F. de Castilhos, *J. Chem. Eng. Data*, **66**, 3512 (2021).
16. W. Y. Tian, Z. X. Zeng, W. L. Xue, Y. B. Li and T. Y. Zhang, *Chinese J. Chem. Eng.*, **18**, 391 (2010).
17. S. C. Li, Z. H. Xi and L. Zhao, *Chem. React. Eng. Technol.*, **5**, 385 (2015).
18. L. W. Chen, J. M. Xu, W. L. Xue and Z. X. Zeng, *Korean J. Chem. Eng.*, **35**, 82 (2018).
19. X. J. Liang, F. J. Wu, Q. L. Xie, Z. Y. Wu, J. J. Cai, C. W. Zheng, J. H. Fu and Y. Nie, *Chinese J. Chem. Eng.*, **44**, 41 (2022).
20. J. C. Jiang, P. Liu, S. Y. Chen, G. D. Feng, J. P. Gong and J. M. Xu, CN Patent, 104496819B (2016).
21. J. G. Wei, D. Z. Liu, P. Q. Sun and S. H. Sun, *J. Chem. Eng. Chinese Univ.*, **20**, 665 (2006).
22. K. Li, J. C. Jiang and X. A. Nie, *Spec. Petrochem.*, **30**, 43 (2013).
23. S. Satoh and T. Sogabe, *Pap. Inst. Phys. Chem. Res.*, **38**, 246 (1941).
24. J. T. Jebbes, *Acta Chem. Scand*, **14**, 180 (1960).
25. K. Schwabe and W. Wagner, *Z. Electrochem*, **65**, 812 (1961).
26. J. D. Cox, D. D. Wagman and V. A. Medvedev, CODATA Key Values for Thermodynamics, *Hemisphere Publishing Corp*, New York (1984).
27. C. L. Yaws, *The YAWS handbook of thermodynamic properties for hydrocarbons and chemicals*, Gulf Pub Co, Houston (2006).
28. V. Růžička and E. S. Domalski, *J. Phys. Chem. Ref. Data*, **22**, 597 (1993).
29. S. W. Benson, F. R. Cruickshank, D. M. Golden, G. R. Haugen, H. E. O'neal, A. S. Rodgers, R. Shaw and R. Walsh, *Chem. Rev.*, **69**, 279 (1969).
30. R. E. Thek and L. I. Stiel, *AIChE J.*, **12**, 599 (1966).
31. P. S. Ma, W. Xu, Y. S. Liu and Y. C. Ruan, *Petrochem. Technol.*, **21**, 613 (1992).
32. J. Marrero-Morejón and E. Pardillo-Fontdevila, *AIChE J.*, **45**, 615 (1999).
33. K. N. P. Rani, T. S. V. R. Neeharika, T. P. Kumar, B. Satyavathi, C. Sailu and R. B. N. Prasad, *J. Taiwan Inst. Chem. Eng.*, **55**, 12 (2015).
34. D. Painer and S. Lux, *Ind. Eng. Chem. Res.*, **58**, 1133 (2019).
35. H. Patel, G. Feix and R. Schomäcker, *Macromol. React. Eng.*, **1**, 502 (2007).
36. K. Okitsu, B. Nanzai, K. Kawasaki, N. Takenaka and H. Bandow, *Ultrason. Sonochem.*, **16**, 155 (2009).
37. A. W. M. Braam and B. J. R. Scholtens, *J. Appl. Polym. Sci.*, **50**, 2007 (1993).

Supporting Information

Pseudo-homogeneous kinetic modeling of dioctyl terephthalate (DOTP) production by esterification of terephthalic acid and 2-ethylhexanol over tetrabutyl titanate catalyst

Feng Zhou, Jinjin Cai, Xiaoning Mao, Zhenyu Wu, and Yong Nie†

Biodiesel Laboratory of China Petroleum and Chemical Industry Federation, Zhejiang Provincial Key Laboratory of Biofuel, and College of Chemical Engineering, Zhejiang University of Technology, Hangzhou 310014, China
(*Received 12 January 2022 • Revised 26 April 2022 • Accepted 28 April 2022*)

Table 1. $\Delta H^0_{fg,\,298.15\,K}$ estimated by Benson method

Group	Contribution value ($kJ \cdot mol^{-1}$)	MEHTP (g)	DOTP (g)	PTA (g)
CH3-(C)	−42.19	2	4	0
CH2-(2C)	−20.64	4	8	0
CH2-(C,O)	−33.91	1	2	0
CH2-(C,CO)	−21.77	0	0	0
CH-(3C)	−7.95	1	2	0
CO-(Cb,O)	−136.07	2	2	2
O-(C,CO)	−180.41	1	2	0
OH-(C)	−158.56	0	0	0
OH-(CO)	−243.2	1	0	2
CbH	13.81	4	4	4
Cb-(CO)	15.49	2	2	2
$\Delta H^0_{fg,\,298.15\,K}$ ($kJ \cdot mol^{-1}$)				
MEHTP (g)		DOTP (g)		PTA (g)
−818.33		−964.34		−672.32

Table 2. $C_{p,\,T}$ estimated by Rozicka and Domalski method

Group	a_i	b_i	d_i	MEHTP	DOTP	PTA (liquid)
CH3-(C)	3.8452	−0.33997	0.19489	2	4	0
CH2-(2C)	2.7972	−0.05497	0.10679	4	8	0
CH2-(C,O)	1.4596	1.4657	−0.2714	1	2	0
CH-(3C)	−0.42867	0.93805	0.0029489	1	2	0
CO-(Cb,O)	16.586	5.4491	−2.6849	2	2	2
O-(C,CO)	−21.434	−4.0164	3.0531	1	2	0
OH-(CO)	−27.587	−0.16485	2.7483	1	0	2
CbH	2.2609	−0.25	0.12592	4	4	4
Cb-(CO)	12.151	−1.6705	−0.12758	2	2	2
$C_{p,\,T}=R(\Sigma n_i a_i+(\Sigma n_i b_i)T/100+(\Sigma n_i d_i)(T/100)^2)$ ($J \cdot mol^{-1} \cdot K^{-1}$)						
	MEHTP		DOTP		PTA (liquid)	
$\Sigma n_i a_i$	37.41		63.47		11.34	
$\Sigma n_i b_i$	3.88		1.53		6.23	
$\Sigma n_i d_i$	1.23		2.08		0.38	

Table 3. T_b and T_c estimated by M-P method

Group	$\Delta T_b'$	$\Delta T_c'$	MEHTP	DOTP	PTA (liquid)
-CH3 and -CH2-	194.25	0.0213	2	4	0
-CH2- and -CH2-	244.88	−0.0206	2	4	0
-CH2- and -CH<	244.14	−0.0134	3	6	0
-CH2- and (-COO)o	475.65	0.0276	1	2	0
(=CH-)r and (=CH-)r (single bond)	285.07	0.2089	1	1	1
(=CH-)r and (=CH-)r (double bond)	112	−0.2246	1	1	1
(=CH-)r and (=C<)r (single bond)	237.22	0.219	2	2	2
(=CH-)r and (=C<)r (double bond)	291.15	−0.3586	2	2	2
(=C<)r and (-COO)c	437.78	0.0241	1	2	0
(=C<)r and -COOH	1,232.55	0.0313	1	0	2
		T_b (K)			T_c (K)
MEHTP		692.13			916.67
DOTP		739.45			969.69
PTA (liquid)		507.66			679.73

Table 4. $\Delta H_{vap,b}$ estimated by Ma method

Group	Δi_0	Δi_1	MEHTP	DOTP	PTA (liquid)
CH3-	−17.52	70.037	2	4	0
-CH2-	190.833	−27.338	5	10	0
=CH-	194.137	118.629	1	2	0
-COOH	385.279	0.158	1	0	2
-COO-	363.706	1,315.35	1	2	0
$(=CH-)_A$	334.843	−201.927	4	4	4
$(=C<)_A$	−77.397	811.464	2	2	2
			$\Delta H_{vap,b}$ (kJ·mol^{-1})		
DOTP		MEHTP		PTA (liquid)	
57.193		66.856		45.999	